AIP Journal of Applied Physics

Photoluminescence lineshape and dynamics of localized excitonic transitions in InAsP epitaxial layers

T. R. Merritt, M. A. Meeker, B. A. Magill, G. A. Khodaparast, S. McGill, J. G. Tischler, S. G. Choi, and C. J. Palmstrøm

Citation: Journal of Applied Physics **115**, 193503 (2014); doi: 10.1063/1.4876121
View online: http://dx.doi.org/10.1063/1.4876121
View Table of Contents: http://scitation.aip.org/content/aip/journal/jap/115/19?ver=pdfcov
Published by the AIP Publishing

Photoluminescence lineshape and dynamics of localized excitonic transitions in InAsP epitaxial layers

T. R. Merritt,[1] M. A. Meeker,[1] B. A. Magill,[1] G. A. Khodaparast,[1,a)] S. McGill,[2] J. G. Tischler,[3] S. G. Choi,[4,b)] and C. J. Palmstrøm[5]
[1]*Department of Physics, Virginia Tech, Blacksburg, Virginia 24061, USA*
[2]*National High Magnetic Field Laboratory, Tallahassee, Florida 32310, USA*
[3]*Naval Research Laboratory, Washington, District of Columbia 20375, USA*
[4]*National Renewable Energy Laboratory, Golden, Colorado 80401, USA*
[5]*Department of Electrical and Computer Engineering, University of California, Santa Barbara, California 93106, USA*

(Received 9 March 2014; accepted 30 April 2014; published online 15 May 2014)

The excitonic radiative transitions of $InAs_xP_{1-x}$ ($x = 0.13$ and $x = 0.40$) alloy epitaxial layers were studied through magnetic field and temperature dependent photoluminescence and time-resolved photoluminescence spectroscopy. While the linewidth and lineshape of the exciton transition for $x = 0.40$ indicate the presence of alloy broadening due to random anion distribution and the existence of localized exciton states, those of $x = 0.13$ suggest that this type of compositional disorder is absent in $x = 0.13$. This localization is further supported by the behavior of the exciton transitions at low temperature and high magnetic fields. $InAs_{0.4}P_{0.6}$ exhibits anomalous "S-shaped" temperature dependence of the excition emission peak below 100 K as well as linewidth broadening at high magnetic fields due to the compression of the excitonic volume amid compositional fluctuations. Finally, photoluminescence decay patterns suggest that the excitons radiatively relax through two channels, a fast and a slow decay. While the lifetime of the fast decay is comparable for both compositions (~30 ps), that of the slow decay increases from 206 ps to 427 ps as x increases from 0.13 to 0.40, attributable to carrier migration between the localization states of $InAs_{0.4}P_{0.6}$. © *2014 AIP Publishing LLC*. [http://dx.doi.org/10.1063/1.4876121]

I. INTRODUCTION

By altering the alloy composition, InAsP ternary alloys are capable of assuming a wide range of band gaps, spanning from 0.35 to 1.35 eV at room temperature. The ability to bandgap engineer in this range is an attractive feature for a variety of optoelectronic applications, most notably for those involving modern optical telecommunication,[1,2] broadband photodetectors,[3] and mid-IR lasers.[4,5] Furthermore, InAsP alloys are capable of assuming a wide range of g-factors; this includes $g = 0$, a desired attribute for semiconductor-based quantum communication applications.[6] Investigating the dynamics of carriers involved in radiative transitions in these alloys not only provides a means to assess and improve sample quality but also aids in the design and optimization of device structures. However, while the morphology and the electronic properties of InAsP have been extensively explored,[7–11,14–17,31] studies concerning optical characterization are limited.[14–17] Although there are a large number of optical studies involving quantum structures,[2,18–20] alloy epilayers are more appropriate when considering fundamental optical transitions since confounding effects, such as quantum confinement and interface-related defects, are avoided.

The optical properties of ternary alloy systems are dominated by excitonic transitions[12] and the behavior of the linewidths associated with those transitions yields important information concerning the quality of the alloy system. For instance, of particular interest is the subject of alloy broadening, in which random distribution of alloy anions leads the broadening of excitonic energy, resulting in larger linewidths than those observed in the binary constituents of the alloy.[13] While there are a few reports on excitonic linewidths in InAsP alloys,[14–17] these studies do not provide a robust treatment of alloy broadening. Huang and Wessels[15] reported full width at half maximum (FWHM) linewidths at 20 K of strain-relaxed $InAs_xP_{1-x}$ alloy epitaxial layers ($0 < x < 0.6$), grown by Metal-Organic Vapor Phase Epitaxy (MOVPE), ranged from 12 to 15 meV. Based on comparisons with excitonic linewidths in InP and X-ray diffraction (XRD) measurements, they concluded that compositional disorder in their samples was minimal. However, a systematic optical study investigating the full character of excitonic localization was not pursued; for instance, the magnetic field and temperature dependencies were not assessed. Magnetic fields have the effect of exacerbating alloy broadening which, in turn, can reveal the extent of compositional disorder, if present.[30] In addition, the localization energy of excitons can be determined from the temperature dependence of exciton emission energy.[35]

In this work, we present experimental investigations into the optical properties of $InAs_xP_{1-x}$ ($x = 0.13$ and $x = 0.40$) epitaxial layers using low temperature photoluminescence (PL) measurements. The nature of anion distribution is assessed from linewidths of excitonic transitions at

a)Author to whom correspondence should be addressed. Electronic mail: khoda@vt.edu
b)The samples studied in this work were grown and characterized as part of S. G. Choi's Ph.D. work at the University of Minnesota.

low temperatures. Furthermore, the temperature evolution of the PL spectra of these epiaxial layers is analyzed to determine the degree of exciton localization. In addition, the effect of applied static magnetic fields on excitonic energies (diamagnetic shift) and linewidths in these alloys is determined. Finally, the excitonic recombination dynamics are discussed in the context of time-resolved PL (TRPL) measurements.

II. EXPERIMENTAL DETAILS

$InAs_xP_{1-x}$ epitaxial layers were prepared by chemical beam epitaxy (CBE) on Fe-doped semi-insulating InP (001) substrates. Further details concerning sample growth are available in Ref. 21. The compositions of the alloys presented in this work, $x = 0.13$ and $x = 0.40$, were verified by high resolution x-ray diffraction measurements using Vegard's rule. XRD rocking curves for $InAs_xP_{1-x}$ with $x = 0.13$ and 0.40 obtained by using CuKa radiation are shown in Fig. 1. By means of ellipsometry, the thicknesses of the epilayers were determined to be 2.2 and 4.3 μm for $x = 0.13$ and $x = 0.40$, respectively. These thicknesses are well beyond the critical thickness for strain relaxation,[7,21] as supported by x-ray reciprocal-space mapping analysis.

PL measurements were performed using an amplified Ti:Sapphire laser as the excitation source, operating at 800 nm with a pulse width of 150 fs and a repetition rate of 1 kHz. Samples were mounted in a 17.5 T superconducting magnet and PL signals were collected through a 0.6 mm core-diameter multimode fiber, delivered to a 0.75 m focal length spectrometer with a 600 grooves/mm grating, and detected by either a liquid-nitrogen-cooled charge-coupled device (CCD) or InGaAs photodiode array. All magnetic field measurements were carried out using a Faraday geometry, in which the direction of the field was perpendicular to the epilayer plane and parallel to the optical excitation. TRPL measurements were performed using a synchroscan streak camera (Hamamatsu Photonics) with a temporal response of 2 ps.

PL spectra were subjected to a nonlinear damped least-squares fitting using Voigt profiles, approximated by a piecewise function involving a Taylor Expansion about precomputed points and a fifth-order Gaussian-Hermite quadrature.[22] Fitted data presented in this work yielded adjusted R^2 values greater than 0.980.

III. RESULTS AND DISCUSSION

Figure 2 shows PL spectra for $InAs_xP_{1-x}$ ternary alloy epitaxial layers measured at 5 K under an excitation fluence of 6 $\mu J/cm^2$. Both spectra involve near band edge transitions, attributable to excitonic transitions (X). The asymmetric excitonic emission for $x = 0.40$ can seemingly be described by two Voigt profiles (see below); however, the profile on the high energy side is an artifact of the high energy tail. This tail feature is indicative of spatial fluctuations in the band gap produced by alloy disorder. Under low energy excitation, the characteristic time needed for carriers to migrate to lower energy sites is shorter than the radiative recombination lifetime; hence, electron-hole pairs preferentially recombine from absolute potential minima, skewing the emission toward the lower energy side.[24]

The spectrum for $x = 0.13$ also possesses an energetically lower, much broader transition. This weaker shoulder has been attributed to free to bound transitions involving a shallow acceptor,[14,15] or a donor-like defect to an acceptor level or valence band transition.[17] When increasing excitation fluence by two orders of magnitude (not shown), this lower energetic transition redshifts, supporting its classification as a donor-acceptor pair (D, A) recombination since Coulomb interaction of donors and acceptors as a function of their separation would lead to a shift in emission energy with excitation density.[23]

In addition, for both compositions, the peak energy and linewidth for the energetically higher transitions did not show an appreciable dependence on excitation density, corroborating our earlier assignment that these peaks are due to excitons. Regarding the excitonic transitions, the peak

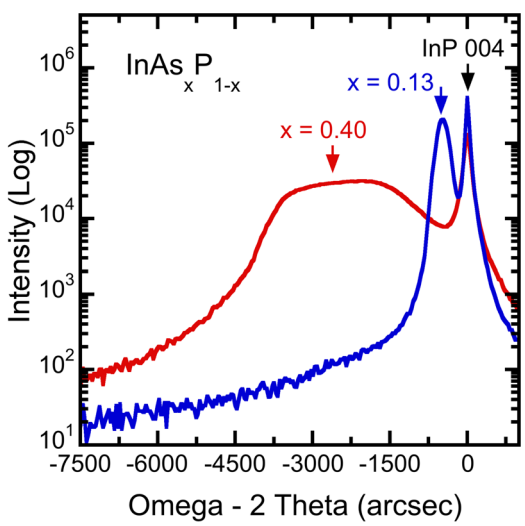

FIG. 1. High-resolution X-ray diffraction rocking curves in the vicinity of the InP 004 reflection for $InAs_xP_{1-x}$ films with $x = 0.13$ (blue line) and 0.40 (red line).

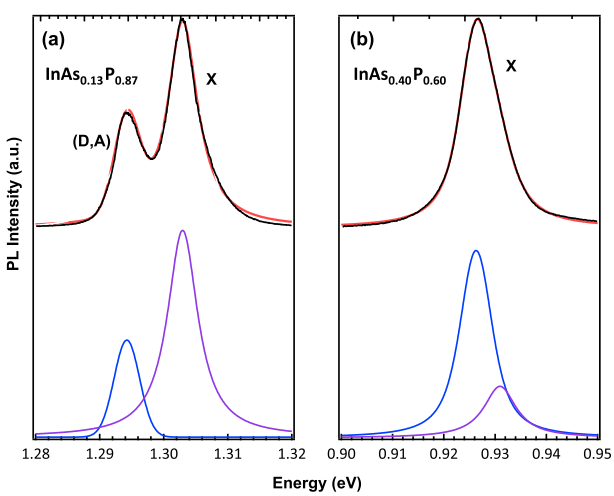

FIG. 2. Photoluminescence spectra for $InAs_xP_{1-x}$ alloy epitaxial layers measured at 5 K with As compositions of (a) 0.13 and (b) 0.40. The fitted spectra (solid red line) overlay experimental values (black lines), and the Voigt profiles that contribute to those fitted spectra are offset below.

energies and FWHM linewidths at 4 K, determined from the fitting protocol, are 1.3030 eV and 5.7 meV for $x = 0.13$, and 0.9263 eV and 7.6 meV for $x = 0.40$. The shift of the excitonic transition toward lower energies with increasing x corresponds to the predicted band gap reduction associated with an increasing As concentration. In contrast, the increase of the linewidth with x suggests the onset of alloy broadening due to random anion distribution.

Through lineshape analysis at low temperatures, the degree of alloy broadening can be assessed, albeit in a limited fashion. Typically, the line shape of bound excitonic optical transitions in binary semiconductors can be approximated as Lorentzian.[24] In contrast, random compositional disorder in alloy semiconductors incurs an inhomogeneous broadening on these transitions, producing lineshapes with a nearly Gaussian profile.[24,34] By performing spectral decomposition of the PL with a function that is the convolution of both profiles, i.e., the Voigt profile, the relative contributions of the various broadening mechanisms can be inferred. The Voigt profile is given by[25]

$$\Phi(u,v) = \frac{1}{\alpha_G}\sqrt{\frac{\ln 2}{\pi}}K(u,v), \tag{1}$$

where $K(u,v)$, known as the "Voigt function," is given by

$$K(u,v) = \frac{v}{\pi}\int_{-\infty}^{\infty}\frac{exp(-t^2)}{v^2+(u-t)^2}dt \tag{2}$$

$$\text{with} \quad u = \frac{\nu-\nu_0}{\alpha_G}\sqrt{\ln 2}, \quad v = \frac{\alpha_L}{\alpha_G}\sqrt{\ln 2},$$

where α_G and α_L are the half-widths of the Gaussian and Lorentzian components, respectively, and $\nu - \nu_0$ is the distance from the profile center.

In Fig. 2, results of this deconvolution analysis are displaced below the observed spectra for $x = 0.13$ and $x = 0.40$. The Lorentzian and Gaussian contribution in each fitted peak can be determined from the shape factor, v, as defined above. According to this definition, a shape factor of zero signifies a Gaussian lineshape; as this factor increases, the Lorentzian component becomes more prominent. The shape factors for the excitonic transitions for $x = 0.13$ and $x = 0.40$ are 28 and 0.8, respectively, indicating that the former can be approximated as Lorentzian whereas the latter is an admixture of the two lineshapes. Since Gaussian broadening is a necessary attribute of alloy broadening due to random anion distribution, the shape factors indicate the possibility of modest alloy broadening in $x = 0.40$ and the lack thereof in $x = 0.13$. However, the linewidth of the excitonic transition in $x = 0.13$, 5.7 meV, is larger than those found in InP (<1 meV) which is typically attributable to homogeneous lifetime broadening. Hence, other Lorentzian-type broadening mechanisms are mostly likely present in the $x = 0.13$ composition.

This finding is further supported by ellipsometric and XRD studies of these structures:[21] The broadening parameters of second-energy-derivative of ellipsometric spectra were larger for mid-compositions ($0.4 < x < 0.6$) than for compositions closer to binary end-points; in addition, as shown in Fig. 1, XRD rocking curves for $x = 0.40$ were broader than those of $x = 0.13$.

The thermal behavior of the PL spectrum is incontrovertibly affected by the distribution of anions within a semiconductor alloy. Fig. 3 shows the lattice temperature dependency of the peak position of the dominant exciton transition for both compositions considered, where these peak positions were determined from the aforementioned fitting protocol. At high temperatures (>100 K), both compositions experience a redshift in peak position with increasing temperature, attributable to the temperature dependence of the band gap, $E_g(T)$. With regard to this thermal dependency, the phonon coupling model proposed by O'Donnell and Chen[26] is more appropriate for describing $E_g(T)$ for $InAs_xP_{x-1}$ alloys than either the Varshini or Bose-Einstein equations.[27] This model asserts that the temperature dependence of the band gap is as follows:

$$E_g(T) = E_g(0) - S\langle h\omega\rangle[\coth(\langle h\omega\rangle/2kT) - 1], \tag{3}$$

where S is a dimensionless coupling constant and $\langle h\omega\rangle$ is the average phonon energy.

The solid lines in Fig. 3 for $x = 0.13$ and $x = 0.40$ represent the nonlinear least squares fit of Eq. (3) with the excitonic peak positions for $T > 100$ K; values of the best fit parameters are given in Table I.

While the thermal behavior of the excitonic peak position for $x = 0.13$ follows closely with that of the band gap well into the low temperature regime, the peak position for

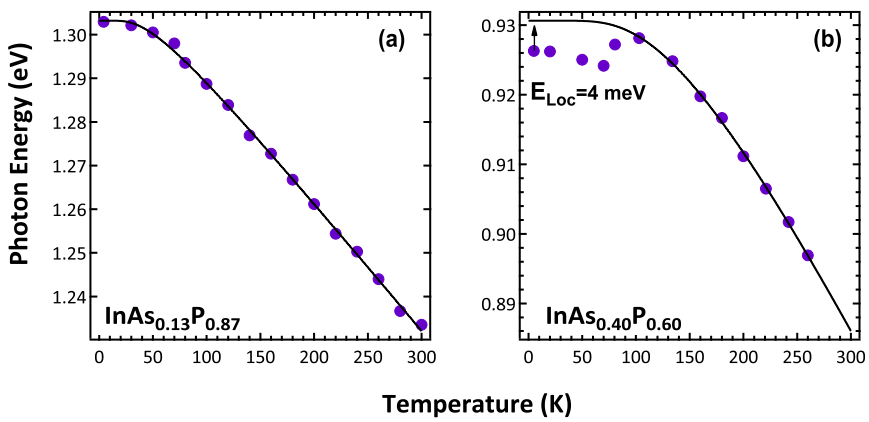

FIG. 3. Temperature dependency of the dominant PL emission peak of $InAs_xP_{1-x}$ for (a) $x = 0.13$ and (b) $x = 0.40$. Solid circles indicate measured values whereas the solid lines denote the best fit of Eq. (3) to the high temperature measurements (>100 K).

TABLE I. Best fit parameters for the high temperature dependence of the dominant PL emission peak for $InAs_xP_{1-x}$.

As concentration (%)	$E_g(0)$ (eV)	S	$\langle \hbar\omega \rangle$ (meV)
13	1.303	1.73	11.4
40	0.930	1.89	36.3

$x = 0.40$ exhibits a markedly different behavior below 100 K. In fact, this divergence from the band gap behavior is known as the thermal "S-shape" emission shift that is prototypical of semiconductor alloy systems with randomly distributed anions.[28] This behavior features a red-blue-red shift of the excitonic peak positions with increasing temperature caused by thermal migration of excitons from localized to delocalized states. The initial redshift occurs when excitons are supplied with sufficient thermal energy to overcome local potential barriers, which allows the excitons to relax into absolute minima. Increasing the lattice temperature further results in the thermal excitation of the excitons into energetically higher extended states; hence, the peaks become blueshifted. At large enough temperatures, ample thermal energy prevents the localization of excitons, at which point any further temperature increase engenders a second redshift in peak positions due to band gap reduction. In other words, the S-shape feature that is present in the peak position temperature dependence for $x = 0.40$ (Fig. 3) is due to a competitive process between localized and delocalized excitonic states and the existence of these localized states is a result of alloy disorder.

Furthermore, at the lowest measurement temperature, the deviation of the peak position from the expected band gap behavior given by Eq. (3) describes the localization energy.[35] At 5 K, E_{Loc} is approximately 4 meV for $x = 0.40$, as indicated in Fig. 3.

Behavior of these excitonic transitions in the presence of a magnetic field can also indicate the extent of the compositional disorder. Fig. 4 shows the evolution of the PL spectra as a function of magnetic field strength for both $InAs_xP_{1-x}$ compositions. Upon the application of a magnetic field, the peak position of the excitonic emission, X, for $x = 0.13$ and $x = 0.40$ experiences a blue shift; in addition, for $x = 0.13$, the impurity transition (D, A) rapidly subsides and the peak position shifts to higher energies.

An explanation for this latter behavior is that, as the magnetic field is increased, the wavefunctions of the localized, impurity states shrink and, as a result, the wavefunction overlap between the states involved in this transition is reduced, thereby, diminishing its oscillator strength. Furthermore, the binding energy of the impurity states decreases at higher fields, prompting a reduction in the number of ionized states at low temperatures; in turn, this both diminishes the peak intensity of and incurs an energetic shift in the impurity transition.

With regard to the excitonic behavior, the excitons undergo a diamagnetic shift to higher energies as a result of Landau quantization.[29] In addition, the linewidth is expected to increase in disordered alloys. This behavior is due to the compression of the excitonic wavefunction under an increasing magnetic field, which causes the lineshape to be more susceptible to the local potential fluctuations resulting from compositional disorder.[34] In turn, this results in a magnetic broadening of the linewidths. While many groups have proposed models to describe the magnetic field dependency of these quantities, we prescribe to the formalism of Mena *et al.* and Lee *et al.*[30,34]

Both employ the same Hamiltonian to describe an exciton in a static magnetic field directed along the z-axis, relying on the symmetric gauge and cylindrical coordinates

$$H = -\nabla^2 + \frac{\gamma}{i}\frac{\partial}{\partial\phi} + \frac{1}{4}\gamma^2\rho^2 - \sqrt{\frac{4}{(\rho^2 + z^2)}} \qquad (4)$$

such that lengths and energies are taken in units of the excitonic radius, $a_{ex} = \epsilon\hbar^2/\mu e^2$, and the effective Rydberg, $R = \hbar^2/2\mu a_{ex}^2$, respectively, where ε is the dielectric constant

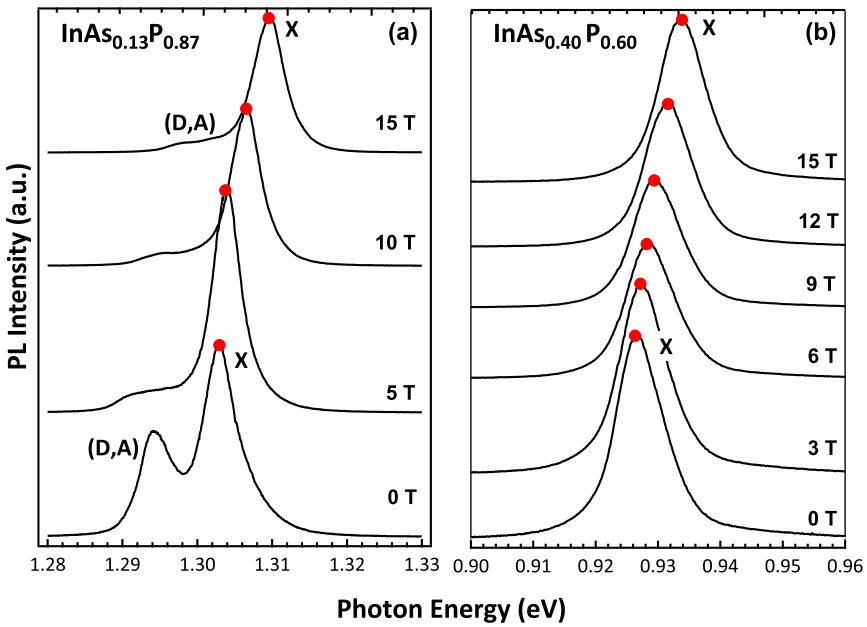

FIG. 4. Magnetic field dependency of the PL spectra for $InAs_xP_{1-x}$ for (a) $x = 0.13$ and (b) $x = 0.40$. The emission peak position (solid circles) for both compositions experiences a blueshift with increasing magnetic field strength, which is the characteristic of a diamagnetic shift. All spectra are normalized and vertically shifted for clarity.

of the alloy and μ is the excitonic reduced mass. The diamagnetic term, $\gamma^2\rho^2/4$, contains the dimensionless parameter γ, which is a measure of the magnetic field strength, defined as $\gamma = \hbar eB/2R\mu c$. The grounds state wavefunction for the Hamiltonian, Eq. (4), was determined through variational calculations using the trial wavefunction

$$\Psi(\rho, z) = A\exp[-\lambda_1\sqrt{\rho^2 + z^2} - \lambda_2\rho^2 + \lambda_3 z^2], \quad (5)$$

where A is the normalization constant, and λ_1, λ_2, and λ_3 are the variational parameters whose values are those that minimize $\langle H\rangle$.

To model the magnetic broadening, the calculations of Mena rely on the expectation value of the excitonic volume; in contrast, Lee[34] relies on a quantum statistical approach. Their derived expressions for linewidths due to compositional variation can be generalized as such

$$\sigma(x) = 2\sqrt{\left(2\ln 2\left(\frac{\partial E_g(x)}{\partial x}\right)^2\Omega(\Psi)\right)}, \quad (6)$$

where $\partial E_g(x)/\partial x$ describes the variation of the direct band gap energy with respect to alloy composition and $\Omega(\Psi)$ is a broadening function that contains the magnetic field dependency. This function assumes the following form:

$$\Omega_{Mena} = \frac{V_c}{a_{ex}^3}\left(\frac{4\pi}{3}\langle\Psi|(\rho^2 + z^2)^{\frac{3}{2}}|\Psi\rangle\right)^{-1}, \quad (7)$$

$$\Omega_{Lee} = \left(\frac{V_c}{a_{ex}^3}\right)^2\sum_{k=-\infty}^{\infty}\sum_{j=1}^{\infty}(2j+1)|\Psi(j\Delta\rho, k\Delta z)|^4, \quad (8)$$

where a is the lattice constant, V_c is the primitive cell volume, and $\Delta\rho$ and Δz are dimensional increments depending on the crystalline structure. For zinc blends, $V_c = a^3/4$, $\Delta\rho = a/\sqrt{2\pi}a_{ex}$, and $\Delta z = a/2a_{ex}$. To calculate $\sigma(x)$ in $InAs_xP_{1-x}$, material parameters from Refs. 21 and 31 were used. Linear interpolation between the properties of InP and InAs was employed to determine the dielectric and lattice constants

$$\epsilon(x) = 12.5(1-x) + 15.2x \quad (9)$$

$$a(x) = 5.87(1-x) + 6.06x\,\text{Å}. \quad (10)$$

The variation of the band gap energy, $\partial E_g(x)/\partial x$, at 4 K in eV is given by

$$\frac{\partial E_g(x)}{\partial x} = -1.09 + 2.4x. \quad (11)$$

Reduced masses were determined experimentally from the diamagnetic shifts exhibited by both compositions. These observed shifts of the peak position with magnetic field were least-squares fit to precomputed curves calculated from the expectation value of the diamagnetic term. Fig. 5 displays the results of this fitting procedure (dashed line) alongside the measured values (solid circles). From the fitted curves, the reduced masses of the excitons in the plane perpendicular to the magnetic field were determined to be $0.048m_0$ and $0.051m_0$ for $x = 0.40$ and $x = 0.13$, respectively, where m_0 is the electron mass in free space. Therefore, the uncertainty in the exciton reduced mass is on the order of $0.001m_0$.

Figure 6 displays the linewidths as a function of magnetic field for the calculated values, solid (Mena) and dashed (Lee) lines, along with the experimental values (solid circles). The magnetic field dependency of the excitonic linewidth for $x = 0.13$ clearly diverges from the expected behavior for alloys with randomly distributed anions. In fact, the reduction of linewidth with an increasing magnetic field is indicative of ordered alloys, where such a behavior is attributed to a diminished exciton-impurity scattering cross section at high magnetic fields.[32]

In contrast, the linewidth for $x = 0.40$ steadily increases with B, albeit displaced from the predicted values by approximately 6 meV. However, the considered models only account for linewidth broadening due to randomly distributed anions and, hence, do not include other broadening mechanisms that would increase the total linewidth beyond the values predicted by both models. For instance, macroscopic compositional disorder such as alloy clustering resulting from spinoidal decomposition would contribute such additional broadening. Furthermore, these macroscopic compositional disorders are more prevalent in mid-composition samples, such as $x = 0.4$, if the growth temperature is not maintained above a critical temperature to discourage local phase separation.[33]

In order to study the radiative dynamics of the exciton transitions, TRPL spectroscopy was employed. Figure 7

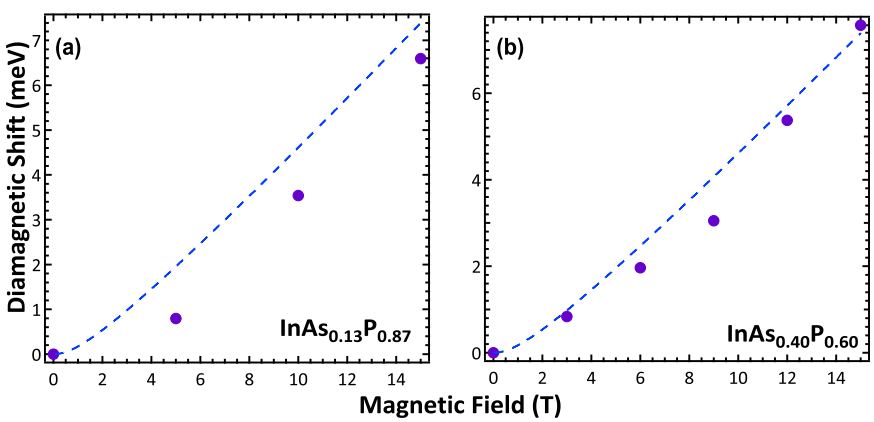

FIG. 5. Variation of the diamagnetic shift of the excitonic transition as a function of magnetic field in $InAs_xP_{1-x}$ for (a) $x = 0.13$ and (b) $x = 0.4$. Experimental values (solid circles) were measured at 5 K and fitted (dashed curve) to pre-tabulated values of $\langle\gamma^2\rho^2/4\rangle$ to determine excitonic reduced masses. For $x = 0.13$ and $x = 0.4$, those reduced masses were determined to be $0.051m_0$ and $0.048m_0$, respectively.

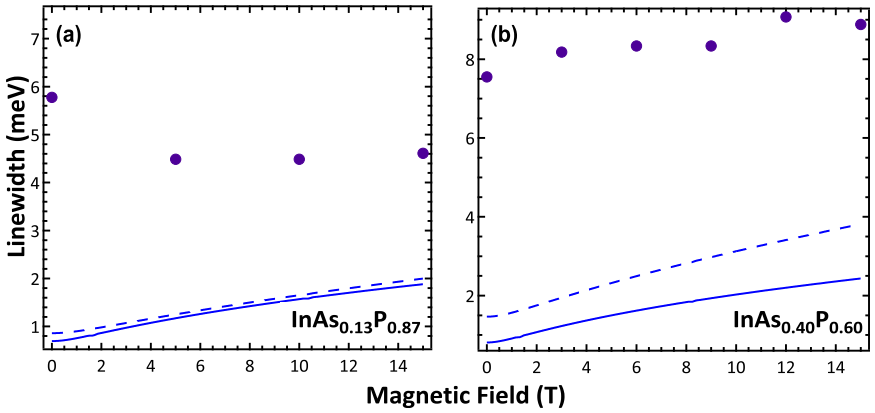

FIG. 6. Variation in the excitonic linewidth for $InAs_xP_{1-x}$ alloy epitaxial layers as a function of magnetic field for As compositions of (a) 0.13 and (b) 0.40. Excitonic linewidths determined from the line shape analysis are represented by solid circles. The dashed and solid lines were produced from the theoretical calculations of alloy broadening on excitonic linewidths according to the derivations of Lee *et al.* and Mena *et al.*, respectively.

shows the temporal response of the PL spectra as a function of temperature for (a) $x = 0.13$ and (b) $x = 0.40$. The TRPL spectra for both compositions feature show a slow and fast decay component. To determine the time scales of these radiative relaxations, the decaying portion of the temporal data was fitted (solid line) to the convolution of the instrument response function and a double-exponential decay function, with the latter being expressed as

$$I(t) = A \exp\left[\frac{-t}{\tau_1}\right] + B \exp\left[\frac{-t}{\tau_2}\right], \tag{12}$$

where τ_1 and τ_2 are time constants for two decay components, and A and B are their relative contributions to the PL intensity. At 0 T and 5 K, τ_1 and τ_2 were 27 and 206 ps for $x = 0.13$, and 28 and 427 ps for $x = 0.40$.

The source of the fast decay component is speculative, but may be due to rapid relaxation of electron-hole pairs through nonradiative pathways, such as surface recombination or Auger cooling. In contrast, the slow decay is most likely the result of a prolonged multistep relaxation process involving carrier cooling through LO-phonon emission and, in the presence of alloy disorder, nonradiative relaxation to energetically low localization states. Due to the low excitation intensities used, cooling excitons give rise to relatively small changes in the LO phonon occupation number such that hot phonon bottlenecking is unlikely.[10] In addition, this carrier migration between localized states may account for the long rise times in the $x = 0.40$ TRPL spectra, depicted by the initial divergence from the fitted behavior.[36,37]

Furthermore, the relaxation of cool excitons may also have to contend with localized states brought about by compositional disorder, which can conceivably account for the two-fold increase in τ_2 for $x = 0.40$ with respect to that for $x = 0.13$. This assertion is based on the fact that localization is analogous to impurity-related binding of excitons and the radiative lifetime of bound excitons increases with binding energy.[35]

This lifetime inflation due to excitonic localization also has a discernible presence in the magnetic field dependency of the TRPL. As mentioned previously, magnetic confinement acts to exacerbate the localization of excitons, which would, in turn, act to increase radiative lifetimes. The right portion of Fig. 8 depicts the dependence of τ_2 on magnetic field strength for $x = 0.13$ and $x = 0.40$, respectively. While τ_2 for $x = 0.13$ remains largely unchanged for $B < 10$ T, the lifetimes for $x = 0.40$ display a noticeable dependence on B, where τ_2 increases from 427 to 459 ps as B increases from 0 to 10 T.

While the lifetimes of the fast decay for both compositions remain relatively unchanged with temperature, the slow decay lifetimes for both $x = 0.13$ and $x = 0.40$ exhibit a marked decrease with increasing temperature, as depicted in the left portion of Fig. 8. Specifically, as the lattice temperature is increased from 5 K to 100 K, τ_2 reduces from 206 to 88 ps for $x = 0.13$, and 427 to 374 ps for $x = 0.40$. This reduction in lifetimes is tenably attributable to the stronger

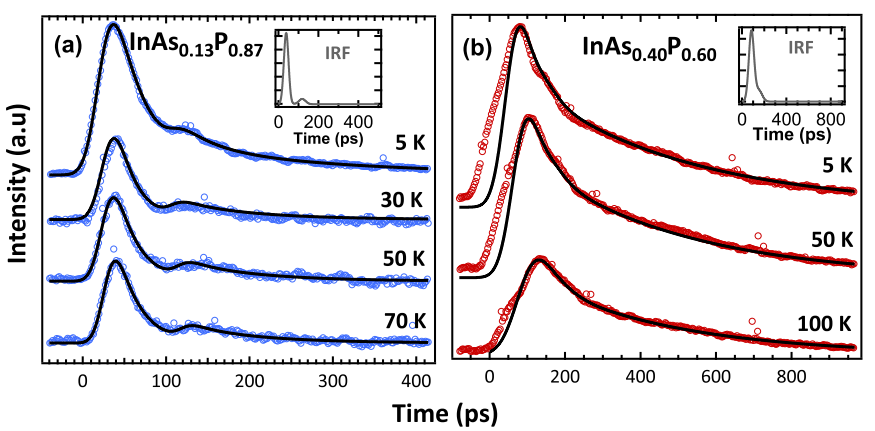

FIG. 7. Temperature-dependent time-resolved PL spectra of $InAs_xP_{1-x}$ for (a) $x = 0.13$ (left) and (b) $x = 0.40$ (right). The decaying portions of the spectra (open circles) were fitted to the convolution of the instrument response function and a double exponential decay function, given in Eq. (12). The insets in both graphs refer to Instrumental Response Function (IRF) deconvolved from the TRPL spectrum for $x = 0.13$ and $x = 0.40$.

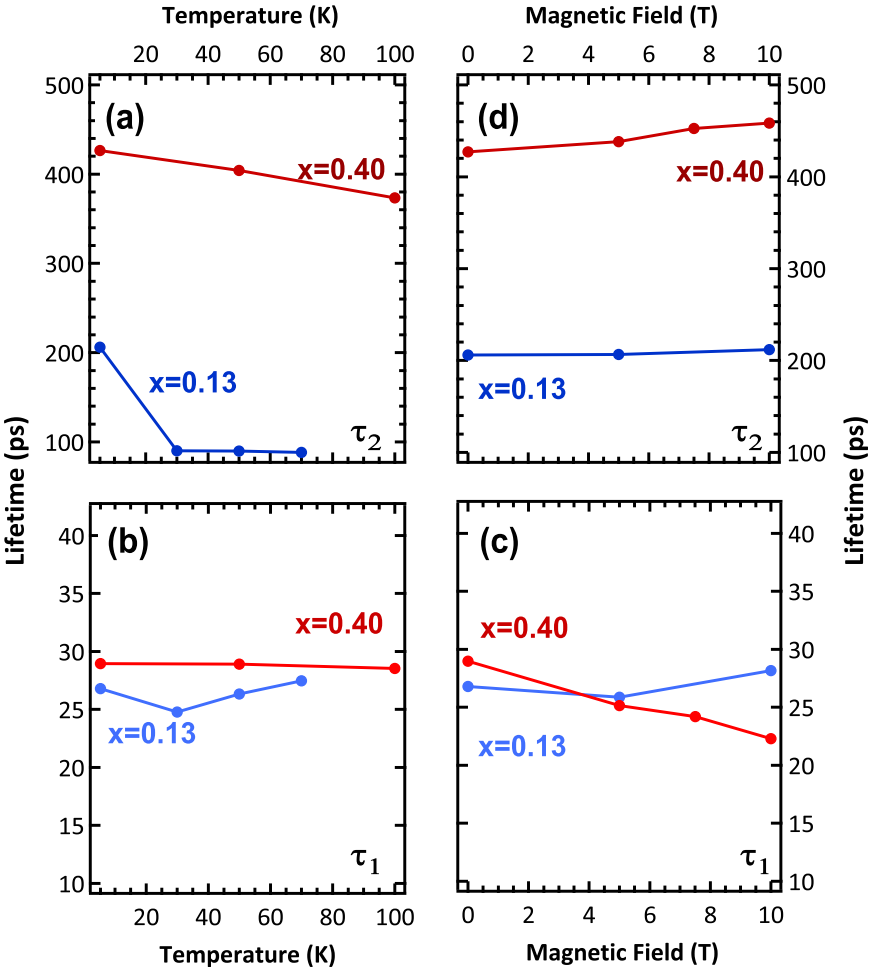

FIG. 8. Temperature ((a) and (b)) and magnetic field ((c) and (d)) dependencies of τ_1 and τ_2, the fast and slow lifetimes of the $InAs_xP_{1-x}$ photoluminescence for $x = 0.13$ and $x = 0.40$. (Starting from the top left corner and proceeding counterclockwise: (a) temperature dependence of τ_2, (b) temperature dependence of τ_1, magnetic field dependence of τ_1, (c) magnetic field dependence of τ_2, and (d) magnetic field dependence of τ_2.)

influence of nonradiative recombination processes and the thermalization of localized states.

IV. CONCLUSIONS

In summary, the excitonic radiative transitions of $InAs_xP_{1-x}$ ($x = 0.13$ and $x = 0.40$) alloy epitaxial layers were studied through magnetic field and temperature dependent photoluminescence and time-resolved PL spectroscopy. The difference in the ionic radius of As and P is larger than that of Al and Ga, then InAs-InP alloys have the microscopic nature quite different from that of AlGaAs alloys. While the linewidth and lineshape of the exciton transition for $x = 0.40$ indicate the presence of alloy broadening due to random anion distribution and the existence of localized exciton states, those of $x = 0.13$ suggest that this type of compositional disorder is absent in this composition. The behavior of the exciton transitions for $x = 0.40$ at low temperatures and high magnetic fields further corroborate this assertion. Below 100 K, the exciton emission peak diverges from the band gap thermal behavior, exhibiting the anomalous "S-shaped" behavior associated with alloy systems possessing exciton localization. From this divergence, the localization energy was determined to be approximately 4 meV. Under high magnetic fields, the $x = 0.40$ linewidth follows the broadening behavior expected for compressed excitonic wavefunctions in the presence of alloy disorder. Finally, the TRPL spectra feature two decay channels for the excitonic radiative transitions. While the lifetime of the fast decay is comparable for both compositions (~30 ps), that of the slow decay increases from 206 ps to 427 ps as x increases from 0.13 to 0.40, attributable to carrier migration between localization states of $x = 0.40$.

ACKNOWLEDGMENTS

This work was supported by NSF-Career Award DMR-0846834, and a portion of this work was performed at the National High Magnetic Field Laboratory, which is supported by NSF Cooperative Agreement No. DMR-1157490, the State of Florida, the U.S. Department of Energy, and through a UCGP. G. A. Khodaparast thanks the inputs from Professor Alexey Belyanin and the funding from the Institute of Critical Technology and Applied Sciences (ICTAS) at Virginia Tech.

[1]Ł. Piskorski, R. P. Sarzała, and W. Nakawaksi, Opto-Electron. Rev. **19**, 320 (2011).
[2]D. Elvira, R. Hostein, F. Bruno, L. Monniello, A. Michon, G. Beaudoin, R. Braive, I. Robert-Philip, I. Abram, I. Sagnes, and A. Beveratos, Phys. Rev. B **84**, 195302 (2011).
[3]M. Wada and H. Hosomatsu, Appl. Phys. Lett. **64**, 1265 (1994).
[4]H. Sugiura, J. Cryst. Growth **164**, 434 (1996).
[5]R. U. Martinelli, T. J. Zamerowksi, and P. A. Longeway, Appl. Phys. Lett. **54**, 277 (1989).
[6]H. Kosaka, A. A. Kiselev, F. A. Baran, K. W. Kim, and E. Yablonovitch, Electron. Lett. **37**, 464 (2001).

[7]S. G. Choi, C. J. Palmstrøm, Y. D. Kim, D. E. Aspnes, H. J. Kim, and Y.-C. Chang, App. Phys. Lett. **91**, 041917 (2007).
[8]M. K. Hudait, Y. Lin, and S. A. Ringel, J. Appl. Phys. **105**, 061643 (2009).
[9]H. Ma, Z. Jin, L. Wang, and G. Ma, J. Appl. Phys. **109**, 023105 (2011).
[10]M. A. Meeker, B. A. Magill, T. R. Merritt, M. Bhowmick, K. McCutcheon, G. A. Khodaparast, J. G. Tischler, S. McGill, S. G. Choi, and C. J. Palmstrøm, Appl. Phys. Lett. **102**, 222102 (2013).
[11]L. Ji, S. L. Lu, Y. M. Zhao, M. Tan, J. R. Dong, and H. Yang, J. Cryst. Growth **363**, 44 (2013).
[12]H. Kaltz, *Optical Properties of III-V Semiconductors* (Springer-Verlag, Berlin, 1996).
[13]K. K. Bajaj, Mater. Sci. Eng. R **34**, 59 (2001).
[14]P. S. Wang and B. W. Wessels, Appl. Phys. Lett. **44**, 766 (1984).
[15]K. H. Huang and B. W. Wessels, J. Cryst. Growth **92**, 547 (1988).
[16]X. Liu, H. Jiang, G. Miao, H. Song, L. Cao, Z. Li, and D. Li, J. Alloys Compd. **506**, 530 (2010).
[17]R. V. Kruzelecky, C. Qiu, and D. A. Thompson, J. Appl. Phys. **75**, 4032 (1994).
[18]H. Q. Hou, C. W. Tu, and S. N. G. Chu, Appl. Phys. Lett. **58**, 2954 (1991).
[19]Y. G. Zhao, R. A. Masut, J. L. Brebner, C. A. Tran, and J. T. Graham, J. Appl. Phys. **76**, 5921 (1994).
[20]C. Y. Lee, M. C. Wu, H. P. Shiao, and W. J. Ho, J. Cryst. Growth **208**, 137 (2000).
[21]S. G. Choi, Ph.D. dissertation, University of Minnesota, 2006.
[22]K. L. Letchworth and D. C. Benner, J. Quant. Spectrosc. Radiat. Transfer **107**, 173 (2007).
[23]Y. H. Cho, G. H. Gainer, J. B. Lan, J. J. Song, W. Yang, and W. Jhe, Phys. Rev. B **61**, 7203 (2000).
[24]E. F. Schubert, E. O. Göbel, Y. Horikoshi, K. Ploog, and H. J. Queisser, Phys. Rev. B **30**, 813 (1984).
[25]B. H. Armstrong, J. Quant. Spectrosc. Radiat. Transfer **7**, 61 (1967).
[26]K. P. O'Donnel and X. Chen, Appl. Phys. Lett. **58**, 2924 (1991).
[27]M. Wada, S. Araki, T. Kudou, T. Umezawa, S. Nakajima, and T. Ueda, Appl. Phys. Lett. **76**, 2722 (2000).
[28]M. Grundmann and C. P. Dietrich, J. Appl. Phys. **106**, 123521 (2009).
[29]M. Hayne and B. Bansal, Luminescence **27**, 179 (2012).
[30]R. A. Mena, G. B. Sanders, K. K. Bajaj, and S. C. Dudley, J. Appl. Phys. **70**, 1866 (1991).
[31]I. Vurgaftman, J. R. Meyer, and L. R. Ram-Mohan, J. Appl. Phys. **89**, 5815 (2001).
[32]S. K. Lyo, E. D. Jones, and S. R. Kurtz, J. Lumin. **60–61**, 409 (1994).
[33]F. Leonard, M. Laradji, and R. C. Desai, Phys. Rev. B **55**, 1887 (1997).
[34]S. M. Lee and K. K. Bajaj, J. Appl. Phys. **73**, 1788 (1993).
[35]H. S. Kim, R. A. Mair, J. Li, J. Y. Lin, and H. X. Jiang, Appl. Phys. Lett. **76**, 1252 (2000).
[36]J. X. Shen, Y. Oka, H. H. Cheng, F. Y. Tsai, and C. D. Lee, Superlattices Microstruct. **25**, 131 (1999).
[37]A. Amo, M. D. Martin, L. Klopotowski, L. Vina, A. I. Toropov, and K. S. Zhuravlev, Appl. Phys. Lett. **86**, 111906 (2005).